Macromolecules

Article

pubs.acs.org/Macromolecules

Construction of Functional Macromolecules with Well-Defined Structures by Indium-Catalyzed Three-Component Polycoupling of Alkynes, Aldehydes, and Amines

Carrie Y. K. Chan,[†] Nai-Wen Tseng,[†] Jacky W. Y. Lam,*[,†] Jianzhao Liu,[†] Ryan T. K. Kwok,[†] and Ben Zhong Tang*[,†,‡,§]

[†]Department of Chemistry, Institute for Advanced Study, Institute of Molecular Functional Materials and Division of Biomedical Engineering, The Hong Kong University of Science and Technology (HKUST), Clear Water Bay, Kowloon, Hong Kong, China

[‡]Guangdong Innovative Research Team, SCUT-HKUST Joint Research Laboratory, State Key Laboratory of Luminescent Materials and Devices, South China University of Technology (SCUT), Guangzhou 510640, China

[§]HKUST-Shenzhen Research Institute, No. 9 Yuexing 1st RD, South Area, Hi-tech Park, Nanshan, Shenzhen 518057, China

Supporting Information

ABSTRACT: We present here a new programmable polymerization route for the synthesis of new conjugated polymers via one-pot reaction route. The three-component polycoupling reactions of terephthalaldehyde and dibenzylamine with 4,4′-diethynyl-1,1′-biphenyl, bis(4-ethynylphenyl)dimethylsilane, 1,2-bis(4-ethynylphenyl)-1,2-diphenylethene, *N*,*N*-bis(4-ethynylphenyl)aniline, or 2,5-bis(4-ethynylphenyl)-1,1-dimethyl-3,4-diphenylsilole are catalyzed by indium(III) chloride in *o*-xylene at 140 °C, affording soluble polymers with well-defined structures and high molecular weights (M_w up to 51 200) in high yields (up to 96.9%). Model reaction was carried out to elucidate the chemical structures of the polymers. The resulting polymers are processable and enjoy high thermal stability. The polymers carrying tetraphenylethene and silole units are weakly emissive in solutions but become strong emitters when aggregated in poor solvents or fabricated as thin films in the solid state, displaying a phenomenon of aggregation-enhanced emission characteristic. Thin films of the polymers show high refractive indices (n = 1.7529−1.6041) in a wide wavelength region of 400−1600 nm with low optical dispersions (D' down to 0.005). The polymers are readily metallified by complexation of their triple bonds with cobalt octacarbonyls. Pyrolysis of the resulting organometallic polymers at high temperature under inert atmosphere generates nanostructured ceramics with high magnetic susceptibility (M_s up to 80.7 emu/g) and near-zero coercivity (H_c down to 0.19 kOe).

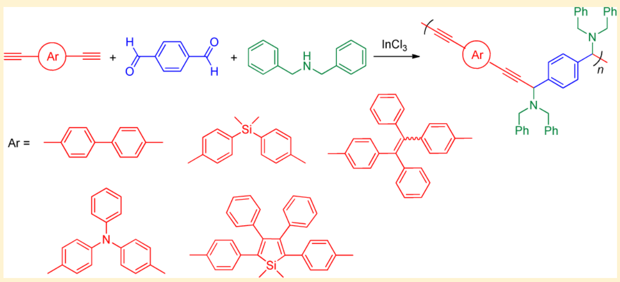

INTRODUCTION

Development of new methodologies for the synthesis of polymers with novel structures and unique properties is a fundamental important area in macromolecular science. Natural polymers such as DNA and protein have well-defined primary structures with ordered sequences of monomer units. In contrast, most synthetic polymers have random structures and are accessed via one- or two-component polymerization route. Some regular polymers have been prepared, but their preparation is difficult and requires skill-demanding techniques such as living polymerization. Development of programmable polymerization reaction is thus of interest because it may generate biomimic polymers with unique materials properties and potential practical applications.

Organic chemists have developed various multicomponent coupling reactions (MCRs) with an aim to access complex compounds or biological-active intermediates from simple precursors. These chemical processes involve three or more reactants for the inherent formation of several covalent bonds in one operation[1] and proceed in chemo- and regioselective fashion with high atom economy[2] and diminution of waste production due to the decrease in the number of synthetic or isolation steps.[3] The transition-metal-catalyzed reaction of alkyne, aldehyde, and amine is one of the representative examples of the MCRs (Scheme 1). Starting from 2002, Li and co-workers discovered one-pot three-component coupling of alkyne, aldehyde, and amine (A^3-coupling) using different types of transition-metal complexes, including Cu−Ru,[4] Co,[5] and Cu.[6] In 2009, efficient indium-catalyzed A^3-coupling via C−H

Scheme 1. Alkyne-Based Three-Component Coupling Reaction

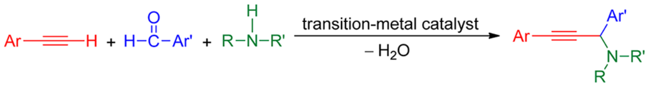

Received: March 13, 2013
Revised: April 12, 2013
Published: April 22, 2013

Scheme 2. Indium-Catalyzed Polycoupling of Diyne, Dialdehyde, and Amine

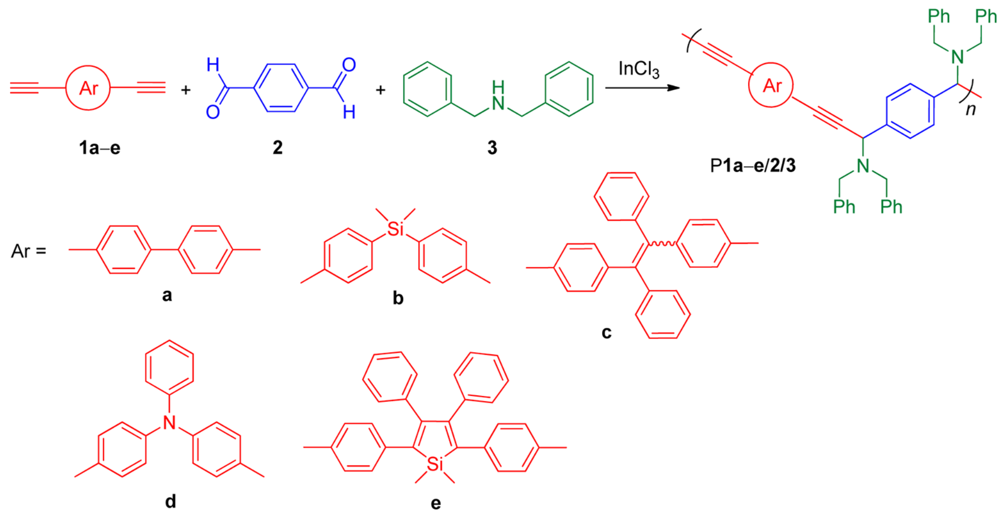

bond activation was reported by Wang.[7] The reaction underwent smoothly without any cocatalyst or activator and afforded the corresponding products in nearly quantitative yields with only water as byproduct.

Despite the advantages of the MCRs, little efforts have been made to develop these organic reactions into useful tools for the synthesis of sequentially well-defined polymers. Tomita and co-workers developed Pd-catalyzed ternary polycondensations to obtain highly functionalized polymers such as poly(arylene vinylene)s containing building blocks originated from three kinds of monomers in high yields.[8] In 2008, Endo et al. discovered three-component polyaddition through combination of chemoselective nucleophilic and radical additions.[9] The polymerization results, however, were not satisfactory. The polydispersity indexes of the polymers were as large as 6.81, though their molecular weights were around 12 000. In 2012, Li et al. reported the one-pot synthesis of polyamides with various functional groups via Passerini reaction of carboxylic acids, dialdehydes, and diisocyanides.[10]

Our research group has been working on the construction of conjugated macromolecules using acetylenic molecules as building blocks.[11] Utilizing monoynes, diynes, and triynes as monomers, we succeeded in the synthesis of a large variety of functionalized polyacetylenes,[12] polydiynes,[13] polyarylenes,[14] polytriazoles,[15] poly(vinylene sulfide)s,[16] poly(silylene vinylene)s,[17] poly(arylene chlorovinylene)s,[18] and poly(arylene ynonylene)s[19] with linear and hyperbranched structures and regio- and stereoregularity by metathesis, cyclotrimerization, coupling, addition, and "click" polymerizations. We found that the polymers showed unique electronic, optical, photonic, mesomorphic, and biological properties, which enabled them to find an array of high-tech applications. In this work, we explore the potential of developing the three-component coupling reaction of alkyne, aldehyde, and amine into versatile alkyne-based polymerization technique for the synthesis of novel polymers with structural regularity and advanced functionality (Scheme 2). Since the new polymers **P1a–e/2/3** possess heteroatoms and unsaturated vinyl and ethynyl units, they are expected to show high refractive indices. The polymers may readily form complexes with metallic species, and the resulting organometallic polymers may serve as processable precursors to magnetic ceramics upon pyrolysis. It is anticipated that polymers with advanced materials properties will find high-tech applications and help sharpen the competitive edge of the technology industries.

■ EXPERIMENTAL SECTION

Materials and Instrumentation. Tetrahydrofuran (THF) was distilled from sodium benzophenone ketyl under nitrogen immediately prior to use. All the chemicals and other reagents were purchased from Aldrich and used as received without further purification. Monomers **1a–e** and 4-ethynylbiphenyl (**8**) were prepared according to the literature procedures.[20] Weight-average molecular weights (M_w) and polydispersities (M_w/M_n) of the polymers were estimated by a Waters gel permeation chromatography (GPC) system equipped with a Waters 515 HPLC pump, a set of Styragel columns (HT3, HT4, and HT6; MW range 10^2–10^7), a column temperature controller, a Waters 486 wavelength-tunable UV–vis detector, a Waters 2414 differential refractometer, and a Waters 2475 fluorescence detector. The polymer solutions were prepared in THF (~2 mg/mL) and filtered through 0.45 μm PTFE syringe-type filters before being injected into the GPC system. THF was used as eluent at a flow rate of 1.0 mL/min. The column temperature was maintained at 40 °C, and the working wavelength of the UV–vis detector was set at 254 nm. A set of monodisperse polystyrene standards (Waters) covering MW range of 10^3–10^7 were used for MW calibration.

^{1}H and ^{13}C NMR spectra were measured on a Bruker AV 300 spectrometer in deuterated chloroform using tetramethylsilane (TMS; δ = 0) as internal reference. High-resolution mass spectra (HRMS) were recorded on a GCT premier CAB048 mass spectrometer operating in MALDI-TOF mode. IR spectra were recorded on a PerkinElmer 16 PC FTIR spectrophotometer. UV spectra were measured on a Milton Ray Spectronic 3000 Array spectrophotometer. Photoluminescence (PL) spectra were recorded on a PerkinElmer LS 55 spectrofluorometer. Fluorescence quantum yields (Φ_F) of thin films of the polymers were measured on a calibrated integrating sphere. Thermogravimetric analysis (TGA) was carried on a TA TGA Q5000 under nitrogen at a heating rate of 10 °C/min. Refractive indices (RI or n) of the polymer films were measured on a prism coupler (Metricon, model PC-2100) equipped with a He–Ne laser light source (wavelengths: 403, 473, 632.8, 934, and 1534 nm). The birefringence (Δn) was calculated as a difference between the n_{TE} (in-plane) and n_{TM} (out-of-plane) values.

X-ray photoelectron spectroscopy (XPS) experiments were conducted on a PHI 5600 spectrometer (Physical Electronics), and the core level spectra were measured using a monochromatic Al Kα X-ray source ($h\nu$ = 1386.6 eV). The analyzer was operated at 23.5 eV pass energy, and the analyzed area was 800 μm in diameter. The energy-dispersion X-ray (EDX) analyses were performed on a JEOL-6300 SEM system with quantitative elemental mapping and line scan

dx.doi.org/10.1021/ma4005346 | Macromolecules 2013, 46, 3246–3256

capacities operating at an accelerating voltage of 15 kV. Structures of the ceramics were investigated on a high-resolution transmission electron microscopy (HRTEM) JEOL 2010F TEM. The X-ray diffractograms were obtained on a Philips PW 2830 powder diffractometer using monochromatized X-ray beam from a nickel-filtered Cu Kα radiation (λ = 1.5406 Å). Magnetization curves were recorded on a Lake Shore 7037/9509-P vibrating sample magnetometer at room temperature.

Preparation of Nanoaggregates. Stock THF solutions of the polymers with a concentration of 10^{-3} M were prepared. Aliquots of the stock solutions were transferred to 10 mL volumetric flasks. After appropriate amounts of THF were added, water was added dropwise under vigorous stirring to furnish 10^{-5} M solutions with different water contents (0−95 vol %). The PL measurements of the resulting solutions were then performed immediately.

Polymer Synthesis. All the polymerization reactions and manipulations were carried out under nitrogen using the standard Schlenk technique in a vacuum line system or an inert atmosphere glovebox (Vacuum Atmosphere), except for the purification of the polymers, which was done in an open atmosphere. The three-component polycoupling reactions were catalyzed by indium(III) chloride in *o*-xylene. A typical experimental procedure for the polycoupling of **1a** with **2** and **3** is given below as an example.

Into a 20 mL test tube equipped with a magnetic stirrer were placed **1a** (0.2 mmol), **2** (0.2 mmol), **3** (0.44 mmol), $InCl_3$ (20 mol %), and 4 Å molecular sieve (∼70 mg) in 2 mL of *o*-xylene. The reaction mixture was stirred on an oil bath at 140 °C under nitrogen for 20 h. The solution was then cooled to room temperature, diluted with 5 mL of chloroform, and added dropwise to 300 mL of methanol/hexane mixture (1:5 v/v) through cotton filter under stirring to precipitate the polymer and meanwhile remove the unreacted monomers and catalytic species. The polymer was filtered by a Gooch crucible, washed with methanol and hexane several times, and dried in vacuum overnight at room temperature to a constant weight.

Characterization Data for P1a/2/3. Yellow solid; yield 96.9% (Table 4, no. 1). M_w 20 440; M_w/M_n 1.66 (GPC, polystyrene calibration). IR (KBr), υ (cm^{-1}): 3061, 3028, 2923, 2884, 2832, 2807, 1662, 1603, 1494, 1453. ^{1}H NMR (300 MHz, $CDCl_3$), δ (TMS, ppm): 7.73, 7.43, 7.31, 4.96, 3.81, 3.57. ^{13}C NMR (75 MHz, $CDCl_3$), δ (TMS, ppm): 140.87, 140.19, 139.12, 133.21, 129.61, 128.99, 127.69, 123.29, 89.04, 86.65, 56.65, 55.39.

P1b/2/3. Yellow solid; yield 94.0% (Table 4, no. 3). M_w 25 940; M_w/M_n 1.76 (GPC, polystyrene calibration). IR (KBr), υ (cm^{-1}): 3061, 3025, 2953, 2830, 2805, 1664, 1594, 1494, 1453. ^{1}H NMR (300 MHz, $CDCl_3$), δ (TMS, ppm): 8.01, 7.72, 7.57, 7.40, 7.28, 4.93, 3.77, 3.51, 0.61. ^{13}C NMR (75 MHz, $CDCl_3$), δ (TMS, ppm): 140.16, 139.81, 139.16, 139.07, 138.98, 134.83, 131.93, 129.58, 128.97, 128.75, 128.40, 127.69, 124.78, 89.27, 86.42, 56.58, 55.35, −1.82.

P1c/2/3. Yellow solid; yield 94.7% (Table 4, no. 4). M_w 30 000; M_w/M_n 2.38 (GPC, polystyrene calibration). IR (KBr), υ (cm^{-1}): 3059, 3027, 2924, 2883, 2831, 2807, 1663, 1601, 1494, 1443. ^{1}H NMR (300 MHz, $CDCl_3$), δ (TMS, ppm): 7.75, 7367, 7.37, 7.25, 7.23, 7.20, 7.12, 4.88, 3.75, 3.72, 3.51. ^{13}C NMR (75 MHz, $CDCl_3$), δ (TMS, ppm): 144.39, 144.30, 144.05, 143.92, 141.56, 140.18, 139.17, 139.09, 132.26, 132.07, 130.26, 129.56, 128.94, 128.72, 128.50, 127.65, 127.48, 122.08, 121.96, 89.31, 86.02, 85.82, 56.54, 55.31.

P1d/2/3. Yellow solid; yield 93.0% (Table 4, no. 5). M_w 22 820; M_w/M_n 2.12 (GPC, polystyrene calibration). IR (KBr), υ (cm^{-1}): 3060, 3027, 2923, 2883, 2831, 2806, 1659, 1594, 1503, 1453, 1318, 1273. ^{1}H NMR (300 MHz, $CDCl_3$), δ (TMS, ppm): 7.72, 7.52, 7.50, 7.41, 7.30, 7.24, 7.20, 7.19, 7.12, 7.11, 4.91, 3.79, 3.76, 3.54, 3.52. ^{13}C NMR (75 MHz, $CDCl_3$), δ (TMS, ppm): 147.98, 147.53, 140.27, 139.31, 139.22, 133.73, 130.26, 129.60, 129.57, 129.10, 128.95, 128.74, 127.67, 125.96, 124.77, 124.20, 117.94, 89.13, 84.99, 56.60, 55.36.

P1e/2/3. Yellow solid; yield 90.0% (Table 4, no. 7). M_w 51 170; M_w/M_n 3.33 (GPC, polystyrene calibration). IR (KBr), υ (cm^{-1}): 3059, 3026, 2952, 2832, 2807, 1602, 1494, 1453, 1293, 1248. ^{1}H NMR (300 MHz, $CDCl_3$), δ (TMS, ppm): 7.96, 7.81, 7.67, 7.39, 7.28, 7.22, 7.07, 6.98, 6.96, 6.86, 4.87, 3.76, 3.72, 3.51, 3.47, 0.55. ^{13}C NMR (75 MHz, $CDCl_3$), δ (TMS, ppm): 155.30, 142.24, 140.60, 140.25, 139.90, 139.21, 132.43, 132.34, 130.63, 129.59, 128.96, 128.34, 127.65, 127.24, 120.99, 89.49, 85.58, 56.55, 55.31, −3.04.

Model Reaction. *N,N*-Dibenzyl-3-(4-biphenylyl)-1-phenylprop-2-ynylamine (**4**) was prepared as a model compound by coupling reaction of 4-ethynylbiphenyl (**8**), benzaldehyde (**9**), and dibenzylamine (**3**). The experimental procedure was similar to that for the syntheses of P**1a**/**2**/**3** described above. White solid; yield 58.3%. IR (KBr), υ (cm^{-1}): 3061, 3027, 2804, 1600, 1489, 1106, 841, 746, 695. ^{1}H NMR (300 MHz, $CDCl_3$), δ (TMS, ppm): 7.76−7.69 (m, 4H), 7.65−7.62 (m, 4H), 7.48−7.44 (m, 6H), 7.39−7.30 (m, 8H), 7.27−7.24 (m, 2H), 4.96 (s, 1H), 3.83−3.79 (d, 2H), 3.58−3.54 (d, 2H). ^{13}C NMR (75 MHz, $CDCl_3$), δ (TMS, ppm): 141.74, 141.11, 140.23, 139.85, 133.07, 129.59, 128.98, 128.81, 128.35, 128.18, 127.79, 127.76, 127.71, 122.84, 89.19, 86.12, 56.80, 55.34. HRMS (MALDI-TOF): *m*/*z* 463.2300 [M$^+$, calcd 463.2303]. Melting point: 125.1 °C.

Metal Complexation. In a typical run for the preparation of cobalt−polymer complex Co−P**1a**/**2**/**3**, 80 mg of P**1a**/**2**/**3** was dissolved under nitrogen in 5 mL of THF in a 30 mL round-bottom flask. 5 mL of a THF solution of $Co_2(CO)_8$ (118.1 mg, 0.34 mmol, or 1.5 mol equiv to the C≡C units of P**1a**/**2**/**3**) was added. The mixture was stirred at room temperature for 1 h, after which the THF solvent was evaporated to about half of its original volume under reduced pressure. The mixture was then added dropwise into a large amount of hexane (∼200 mL) through a cotton filter under stirring. The precipitates were washed with hexane for three times and dried under vacuum to a constant weight. 140.3 mg of brown solid was obtained. IR (KBr), υ (cm^{-1}): 2089, 2051, 2025 (C≡O).

Co−P1b/2/3. It was prepared from 80 mg of P**1b**/**2**/**3** with $Co_2(CO)_8$ (108.7 mg, 0.32 mmol). Brown solid (126.9 mg). IR (KBr), υ (cm^{-1}): 2089, 2052, 2026 (C≡O).

Co−P1c/2/3. It was prepared from 60 mg of P**1c**/**2**/**3** with $Co_2(CO)_8$ (70.3 mg, 0.20 mmol). Brown solid (96.6 mg). IR (KBr), υ (cm^{-1}): 2088, 2051, 2025 (C≡O).

Co−P1d/2/3. It was prepared from 80 mg of P**1d**/**2**/**3** with $Co_2(CO)_8$ (104.2 mg, 0.30 mmol). Brown solid (147.7 mg). IR (KBr), υ (cm^{-1}): 2088, 2050, 2023 (C≡O).

Co−P1e/2/3. It was prepared from 60 mg of P**1e**/**2**/**3** with $Co_2(CO)_8$ (64.3 mg, 0.19 mmol). Brown solid (97.6 mg). IR (KBr), υ (cm^{-1}): 2088, 2051, 2025 (C≡O).

Pyrolytic Ceramization. Ceramics MC**1**−MC**5** were fabricated from the precursors Co−P**1a**−**e**/**2**/**3** by pyrolysis in a Lindberg/Blue tube furnace with a heating capacity up to 1700 °C. In a typical ceramization experiment, 100 mg of Co−P**1a**/**2**/**3** was placed in a porcelain crucible, which was heated to 1000 °C at a heating rate of 10 °C/min under a steam of nitrogen (0.2 L/min). The sample was sintered for 1 h at 1000 °C, and black ceramic MC**1** was obtained in 45.9% yield (45.9 mg) after cooling.

■ RESULTS AND DISCUSSION

Polymerizatiom Reaction. To explore the one-pot A^3-coupling of diyne, dialdehyde, and secondary amine into a useful tool for the preparation of sequentially well-defined polymers, we prepared a group of functional diynes (**1a**−**1e**) according to our previous published papers.[20] On the other hand, terephthalaldehyde **2** and dibenzylamine **3** were commercially available and purified before use.

To search for optimum conditions for the polymerization, we first studied the solvent effect on the A^3-coupling reaction using 4,4′-diethynyl-1,1′-biphenyl (**1a**), **2**, and **3** as monomers. The polymerization was carried out in the presence of indium(III) chloride at high temperature for 20 h under inert atmosphere. As shown in Table 1, the solvent exerts strong effect on the reaction. Among the tested solvents, *o*-xylene was the most suitable medium for the polycoupling reaction, giving a soluble polymeric product with the highest molecular weight (M_w = 17 400) in the highest yield (99.3%) (Table 1, no. 6). Satisfactory results are also obtained in benzene, 1,2-dichloroethane, and

Table 1. Solvent Effect on the Polymerization of 1a with 2 and 3[a]

entry	solvent	temp (°C)	yield (%)	M_w[b]	M_w/M_n[b]
1	benzene	80	81.5	9500	1.8
2	DCE	80	82.1	6200	1.4
3	acetonitrile	80	trace		
4	dioxane	100	0		
5	toluene	120	80.0	7700	1.6
6	*o*-xylene	140	99.3	17400	2.4
7	*o*-DCB	140	45.0	5700	1.6
8	benzonitrile	140	28.6	4700	1.4

[a]Carried out under nitrogen for 20 h. [**1**] = [**2**] = 0.067 M, [**3**] = 0.133 M, [$InCl_3$] = 0.013 M. Abbreviation: DCE = 1,2-dichloroethane, *o*-DCB = 1,2-dichlorobenzene. [b]Determined by GPC in THF on the basis of a polystyrene calibration.

toluene. Polymers with much lower molecular weights, however, are isolated in lower yields when the polymerizations were carried out in 1,2-dichlorobenzene and benzonitrile. Acetonitrile and 1,4-dioxane are nonsolvents for the polymerization as no or trace amount of polymeric products are produced in these solvents.

We are then investigated the temperature effect on the polymerization in *o*-xylene. At low temperature, no or trace amount of polymer was obtained (Table 2, no. 2 and 3). At temperature close to the boiling point of *o*-xylene, a high molecular weight polymer was obtained in nearly quantitative yield. Clearly, the polymerization proceeds only when sufficient energy is provided.

Table 2. Temperature Effect on the Polymerization of 1a with 2 and 3[a]

entry	temp (°C)	yield (%)	M_w[b]	M_w/M_n[b]
1	100	0		
2	120	65.0	5100	1.5
3[c]	140	99.3	17400	2.4

[a]Carried out under nitrogen in *o*-xylene for 20 h. [**1**] = [**2**] = 0.067 M, [**3**] = 0.133 M, [$InCl_3$] = 0.013 M. [b]Determined by GPC in THF on the basis of a polystyrene calibration. [c]Data taken from Table 1, no. 6.

Control of stereoselectivity in the polymerization process is very important for the synthesis of polymers with precise structures. With respect to the catalyst loading, 0.013 M of $InCl_3$ is found to be optimal. However, no significant improvement in the polymerization result was observed when double amount of $InCl_3$ was used for the polycoupling reaction (Table 3, no. 3). Theoretically, the molar ratio between **1**, **2**, and **3** should be in 1:1:2. To see whether it is really the case, the concentration effect of **3** on the polymerization was evaluated. However, neither lower (0.120 M) nor higher (0.173 M) concentration of **3** is good for the polymerization. Instead, a slightly excess amount of **3** (0.146 M) is enough to give a soluble polymer with a high molecular weight in a high yield (96.9%).

Table 3. Concentration Effect on the Polymerization of 1a with 2 and 3[a]

entry	[3] (M)	[$InCl_3$] (M)	yield (%)	M_w[b]	M_w/M_n[b]
1	0.120	0.013	98.0	10100	2.0
2[c]	0.133	0.013	99.3	17400	2.4
3	0.133	0.026	97.8	17400	2.2
4	0.146	0.013	96.9	19500	2.5
5	0.173	0.013	80.2	8400	1.8

[a]Carried out under nitrogen in *o*-xylene at 140 °C for 20 h. [**1**] = [**2**] = 0.067 M. [b]Determined by GPC in THF on the basis of a polystyrene calibration. [c]Data taken from Table 1, no. 6.

Table 4. Polymerization 1a–e with 2 and 3[a]

entry	monomer	yield (%)	M_w[b]	M_w/M_n[b]
1	**1a**	96.9	19 500	2.5
2	**1b**	71.7	20 400	1.7
3[c]	**1b**	94.0	25 900	1.8
4	**1c**	94.7	30 000	2.4
5	**1d**	93.0	22 800	2.1
6	**1e**	80.7	32 800	2.4
7[c]	**1e**	90.0	51 200	3.3

[a]Carried out under nitrogen in *o*-xylene at 140 °C for 20 h. [**1**] = [**2**] = 0.067 M, [**3**] = 0.146 M, [$InCl_3$] = 0.013 M. [b]Determined by GPC in THF on the basis of a polystyrene calibration. [c][**1**] = [**2**] = 0.1 M, [**3**] = 0.22 M, [$InCl_3$] = 0.02 M.

The above investigation allows us to polymerize other monomer combination under optimum conditions. Table 4 summarizes the polymerization results. All the polymerizations proceed smoothly, giving polymers in high yields (71.7–94.7%) with high molecular weights (M_w = 20 400–32 800). The polymerization of **1b** or **1e** with **2** and **3** carried out at higher reactant concentrations gives much better results: polymers with higher molecular weights up to 51 200 are isolated in higher yields up to 94.0%.

Synthesis of Model Compound. To confirm the occurrence of the A^3-polycoupling and gain insights into the chemical structures of the polymers, we performed a model reaction as shown in Scheme 3. 4-Trimethylsilylbiphenyl (**7**) was prepared by lithium-mediated halogen-exchange reaction of 4-bromobiphenyl (**5**), followed by palladium-catalyzed Sonogashira coupling of **6** with trimethylsilylacetylene. Subsequent removal of the trimethylsilyl group of **7** in alcoholic K_2CO_3 solution generated the desirable product **8**. Compound **8** was then reacted with commercially available benzaldehyde (**9**) and dibenzylamine (**3**) in the presence of $InCl_3$ at 140 °C in *o*-xylene to afford *N*,*N*-dibenzyl-3-(4-biphenylyl)-1-phenylprop-2-ynylamine (**4**). The model compound **4** was characterized by standard spectroscopic techniques from which satisfactory analysis data corresponding to its expected molecular structure were obtained (see Experimental Section for details).

Structural Characterization. The polymeric products were characterized spectroscopically. The IR spectrum of P**1a**/**2**/**3** is given in Figure 1 as an example. The spectra of its monomers (**1a**, **2**, and **3**) and model compound **4** are also shown in the same figure for the purpose of comparison. The absorption bands observed at 3237, 1693, and 3326 cm^{-1} are associated with the ≡C–H, C═O, and N–H stretching vibrations of **1a**, **2**, and **3**, respectively. The bands, however, are not observed in the spectrum of P**1a**/**2**/**3**, which is suggestive of the occurrence of the polymerization.

Figure 2 shows the ^{1}H NMR spectra of P**1a**/**2**/**3**, its monomers (**1a**, **2**, and **3**), and model compound **4**. The spectrum of P**1a**/**2**/**3** shows no peaks at δ 3.14, 10.14, and 3.74, which are assigned to the resonances of the acetylene, aldehyde, and methylene protons of **1a**, **2**, and **3**, respectively. Instead, three new peaks emerge at δ 4.96, 3.81, and 3.57. By comparing

Scheme 3. Synthetic Route to Model Compound 4

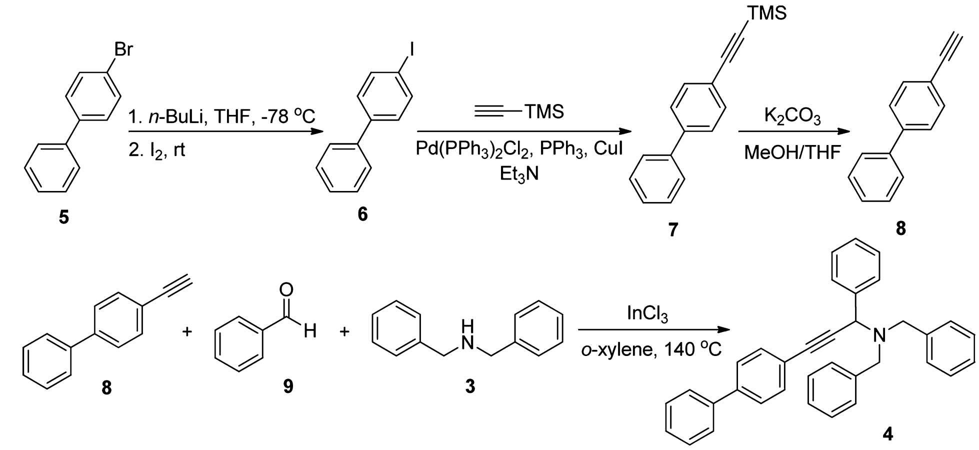

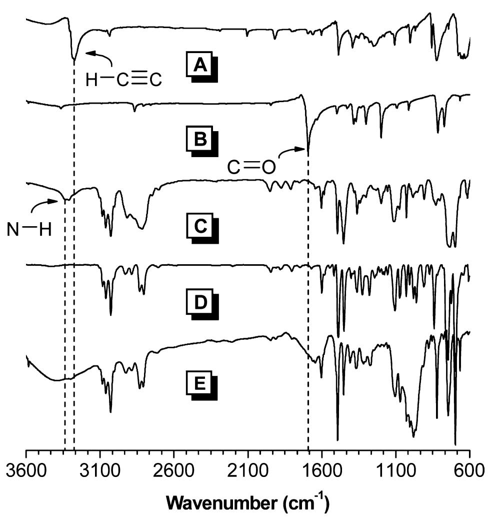

Figure 1. FT-IR spectra of (A) **1a**, (B) **2**, (C) **3**, (D) model compound **4**, and (E) polymer P**1a**/**2**/**3**.

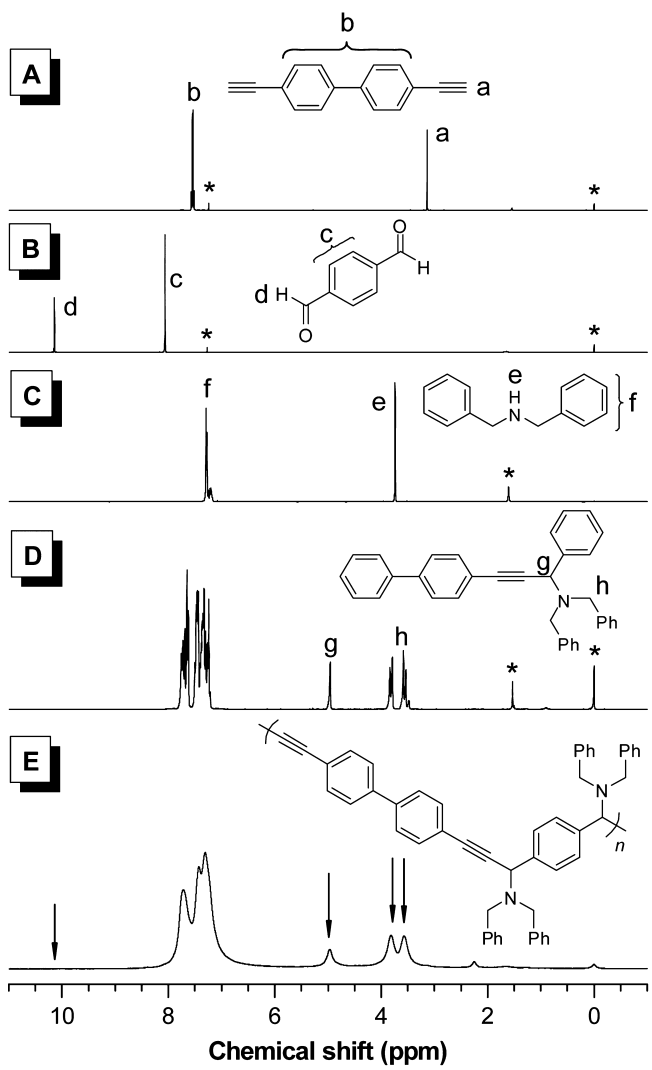

Figure 2. ^{1}H NMR spectra of (A) **1a**, (B) **2**, (C) **3**, (D) model compound **4**, and (E) polymer P**1a**/**2**/**3** in chloroform-*d*. The solvent peaks are marked with asterisks.

with the model compound, these peaks are associated with the resonances of the methylene protons connected to the nitrogen atom. The absorption peaks of P**1a**/**2**/**3** are much broader than those of **4**, indicative of its polymeric nature.

The ^{13}C NMR spectrum of P**1a**/**2**/**3** displays no resonance peak of carbonyl carbon of **2** at δ 192.2. The resonances of the acetylenic carbon atoms of **1a**, however, shift from δ 83.4 and 78.1 to δ 89.0 and 86.6 after the polymerization. New peaks due to the resonances of the methylene carbons next to the nitrogen atom of **3** occur at δ 56.6 and 55.4. These results demonstrate the precise structure of the polymer and are well consistent with the results from IR and ^{1}H NMR analyses.

Solubility and Thermal Stability. All the polymers possess good solubility in common organic solvents, such as dichloromethane, chloroform, tetrahydrofuran, and dioxane. They also possess good film-forming ability and can be readily fabricated into tough solid films by spin-coating and static-casting processes. The thermal properties of the polymers are evaluated by TGA analysis. As shown in Figure 4, all the polymers enjoy high thermal stability, exhibiting 5% weight loss at temperature (T_d) from 249 to 281 °C. They also carbonize in moderate yields up to 50% when they are heated to 800 °C.

Optical Properties. Figure 5 shows the UV spectra of P**1a**−**e**/**2**/**3** in dilute THF solutions. The absorption spectra vary with the polymer structures and are peaked at 301−377 nm. Among the polymers, the absorption maximum of P**1e**/**2**/**3** is located at the longest wavelength, revealing that it possesses the highest electronic conjugation. The photo-

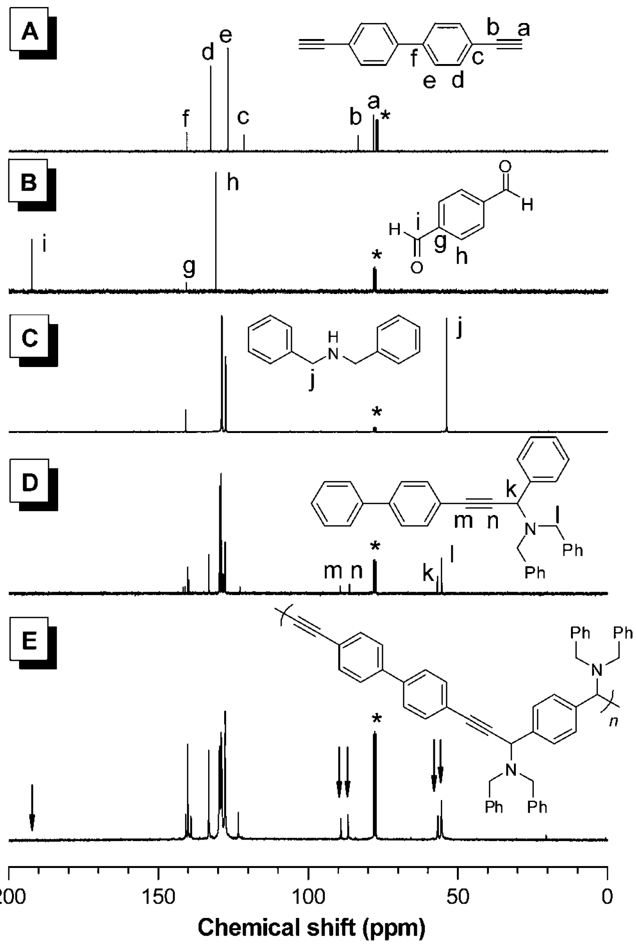

Figure 3. ^{13}C NMR spectra of (A) **1a**, (B) **2**, (C) **3**, (D) model compound **4**, and (E) polymer P**1a**/**2**/**3** in chloroform-*d*. The solvent peaks are marked with asterisks.

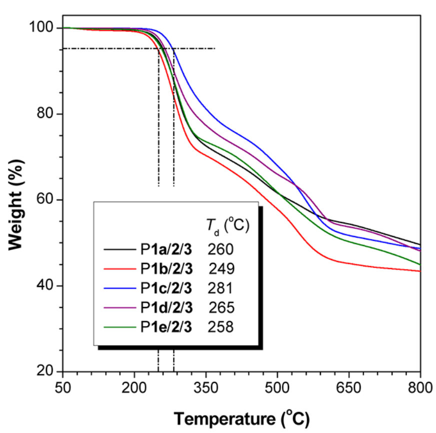

Figure 4. TGA thermograms of P**1a**–**e**/**2**/**3** recorded under nitrogen at a heating rate of 10 °C/min.

luminescence (PL) spectra of P**1a**–**e**/**2**/**3** in dilute THF solutions are centered at 385–509 nm, whereas those of amorphous films are observed at the longer wavelengths of 486–590 nm (Table 5).

Conventional luminescent polymers often suffer from strong interstrand interaction in the aggregated state, which quenches and red-shifts their light emission.[21] In the present work, a similar phenomenon was also observed in P**1a**/**2**/**3** and P**1d**/**2**/**3**. Their fluorescence quantum yields (Φ_F) determined in THF solutions using 9,10-diphenylanthracene (Φ_F = 90% in cyclohexane) as standard are 7.9 and 10.9%, respectively, whose values become much lower (Φ_F = 3.3 and 5.5%) when they are fabricated as thin films in the solid state. Such aggregation-caused quenching (ACQ) effect poses an obstacle to the development of efficient light emitters utilized as thin films in real-world applications. We observed an exact opposite phenomenon of aggregation-induced emission (AIE): a group of propeller-like luminogenic molecules such as tetraphenylethene (TPE) and hexaphenylsilole are nonemissive in solutions but emit intensely in the aggregated state.[22] The AIE effect enables the luminogens to serve as excellent light-emitting materials for organic light-emitting diodes with external quantum efficiency close to the theoretical limit.[22,23] Current study mainly focuses on small AIE molecules with twisted structures. To overcome the processing disadvantage of low molecular weight compound, in this project, we synthesized TPE and silole-containing diynes (**1c** and **1e**) in order to prepare new luminescent polymers with high solid-state Φ_F values.

Figure 6 depicts the change in the PL spectra of P**1c**/**2**/**3** and P**1e**/**2**/**3** in THF solutions upon water addition. In diluted THF solution (10 μM), P**1c**/**2**/**3** emits a bluish-green light at 503 nm. Gradual addition of water, a nonsolvent for the polymer, into its THF solution has progressively enhanced its light emission without any change in the spectral profile, demonstrating a phenomenon of aggregation-enhanced emission (AEE). Similar observation was found in P**1e**/**2**/**3**. However, when more than 80% of water was present in the THF solution, the suspension became unstable and favored the formation of aggregates with "larger" sizes. This has lowered the effective concentration of the solution and hence the PL intensity. To have a quantitative concept, the Φ_F values of P**1c**/**2**/**3** and P**1e**/**2**/**3** in the solution state are measured. The calculated values (1.5 and 2.9%) are much lower than those in the solid thin film state (14.3 and 11.6%). Clearly, the polymers are AEE-active.

We have proposed that restriction of intramolecular rotation (RIR) is the main cause for the AIE effect.[22] In the solution state, the intramolecular rotation is active, which serves as nonradiative pathways for the excitons to decay. In the aggregated state, such rotation is restricted, which blocks the relaxation channels and thus turns on the light emission of the luminophore. The TPE and silole units in P**1c**/**2**/**3** and P**1e**/**2**/**3** are linked together by covalent bonds, which have partially restricted their rotation and hence made the polymers somewhat emissive in THF solution. In THF/water mixture, the RIR process is further activated, which has further enhanced the light emission. Demonstratively, the present results provide good examples on how to build highly emissive polymers with good spectral stability in the aggregated state.

Light Refraction. Macroscopically processable polymers with high refractive index (RI or n) are promising candidate materials for an array of photonic applications, such as lenses, prisms, waveguides, memories, and holographic image recording systems.[24] From the structural point of view, P**1a**–**e**/**2**/**3** consist of polarizable aromatic rings, acetylene units, and heteroatoms and thus may show high light refractivity. Indeed, P**1a**–**e**/**2**/**3** show high RI values of 1.7443–1.6200, 1.6845–1.6052, 1.7529–1.6178, 1.7202–1.6180, and 1.6979–1.6041, respectively, in a wide spectral region of 400–1600 nm. All the polymers exhibit RI values higher than 1.60 from visible to

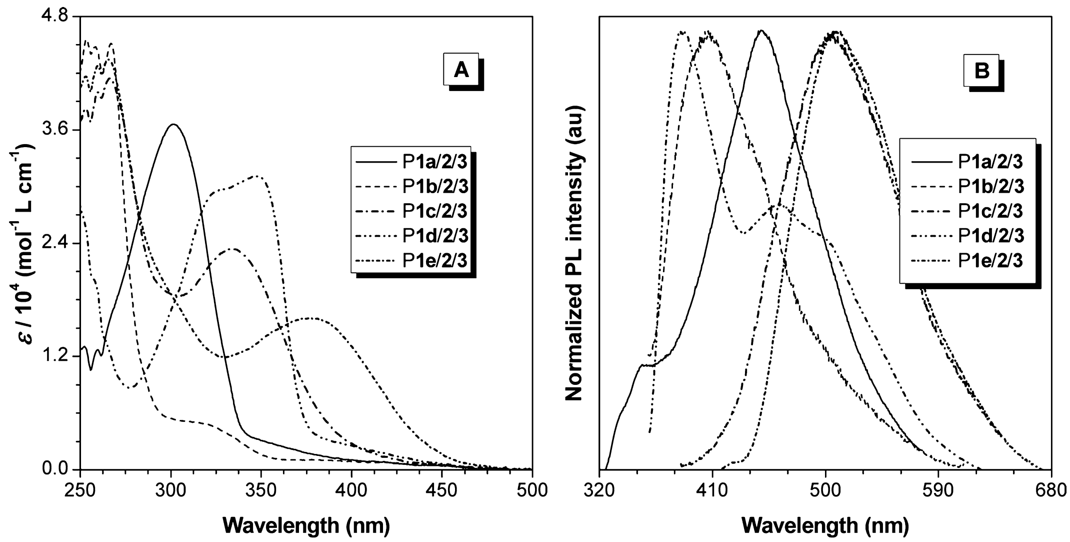

Figure 5. (A) UV and (B) PL spectra of P1a−e/2/3 in THF solutions. Solution concentration: 10^{-5} M; excitation wavelength (nm): 300 (P1a/2/3), 320 (P1b/2/3), 335 (P1c/2/3), 350 (P1d/2/3), and 380 (P1e/2/3).

Table 5. Optical Properties of P1a−e/2/3 in Solution (Soln),[a] Aggregated (Aggr),[b] and Amorphous (Amor)[c] States

	λ_{ab}[d] (nm)	λ_{em}[e] (nm)		
polymer	Soln	Soln ($\Phi_{F,S}$)	Aggr	Amor ($\Phi_{F,F}$)
P1a/2/3	301	449 (7.9)		486 (3.3)
P1b/2/3	317	407 (2.1)		590 (3.7)
P1c/2/3	333	503 (1.5)	503	516 (14.3)
P1d/2/3	347	385, 464 (10.9)		550 (5.5)
P1e/2/3	377	509 (2.9)	512	528 (11.6)

[a]In dilute THF solution (10 μM). [b]In THF/H_2O mixture (1:9 by volume). [c]In solid thin film. [d]Absorption maximum. [e]Emission maximum with quantum yields (Φ_F, %) given in the parentheses. $\Phi_{F,S}$ = fluorescence quantum yield in THF solution determined using 9,10-diphenylanthracene (Φ_F = 90% in cyclohexane) as standard; $\Phi_{F,F}$ = fluorescence quantum yield for thin film measured by a calibrated integrating sphere.

infrared light region, which are much higher than those of the conventional polymers,[25] such as polystyrene (n = 1.602−1.589), poly(methyl methacrylate) (n = 1.497−1.489), and polycarbonate (n = 1.593−1.576). Low birefringence (down to 0.008 at a wavelength of 633 nm) is detected. Evidently, these results highlight the feature of high refractivity of our polymers.

Chromatic Dispersion. For a material to be useful for technological applications, its chromatic aberration should be small. The Abbé number (ν_D) of a material is a measure of the variation or dispersion in its RI with wavelength and is defined as $\nu_D = (n_D - 1)/(n_F - n_C)$, where n_D, n_F, and n_C are the RI values at Fraunhofer D, F, and C lines of 589.3, 486.1, and 656.3 nm, respectively.[26] A modified Abbé number (ν_D') has been proposed to evaluate the application potential of an optical material, using its RI values at the nonabsorbing infrared wavelengths of 1064, 1319, and 1550 nm. The modified Abbé number is defined as $\nu_D' = (n_{1319} - 1)/(n_{1064} - n_{1550})$, where n_{1319}, n_{1064}, and n_{1550} are the RI values at 1319, 1064, and 1550 nm, respectively. The optical dispersions D and D' in the visible and infrared regions are the reciprocals of ν_D and ν_D' and are defined as $D^{(')} = 1/\nu_D^{(')}$.

As shown in Table 6, the ν_D and ν_D' values of P1/2/3 lie in the range of 18.4−32.1 and 52.7−208.5, corresponding to D and D' values of 0.031−0.054 and 0.005−0.019, respectively. The low optical aberrations of the polymers coupled with their high optical transparencies and light refractivities may enable them to find technological applications as coating materials in the advanced optical display systems, such as microlens components for charge-coupled devices and high-performance CMOS image sensors.[24]

Metal Complexation. Organometallic polymers are hybrid macromolecules of organic and inorganic species and exhibit unique magnetic, electronic, catalytic, sensoric, and optical properties.[27] They are also potential candidates as precursors for the fabrication of nanostructured materials and advanced ceramics.[28] Acetylene triple bond is a versatile ligand and commonly used in organometallic chemistry.[29] Polymers P1a−e/2/3 contain numerous triple bonds and should be readily metallified through complexation with organometallic compounds. When mixtures of P1a−e/2/3 and octacarbonyldicobalt with a $[Co_2(CO)_8]/[C{\equiv}C]$ ratio of 1.5:1 were stirred in THF at room temperature, the solution darkened in color accompanying with gas evolution. The mixture remained homogeneous until the end of reaction and Co−P1a−e/2/3 were obtained by precipitation of the reaction mixtures into hexane (Scheme 4). Although the cobalt-containing P1a−e/2/3 dissolved readily during the complexation reaction, they became insoluble after purification, probably due to the formation of supramolecular aggregates during the precipitation and the drying processes. Comparing the IR spectrum of P1a/2/3 with that of its organometallic counterpart, new, strong bands of typical cobalt carbonyl absorption appear at 2089, 2051, and 2025 cm^{-1}, indicative of the integration of the metallic species into the polymer structure at the molecular level.

Pyrolytic Ceramization. The organometallic polymers are pyrolyzed at 1000 °C for 1 h under nitrogen, which give MC1−MC5 in satisfactory yields (45.9−51.1%) (Scheme 4). They are magnetizable and can be readily attracted by a bar magnet, encouraging us to study their properties.

Structure and Composition. The structures of MC1−MC5 are investigated by TEM. As depicted in Figure 9A,B and

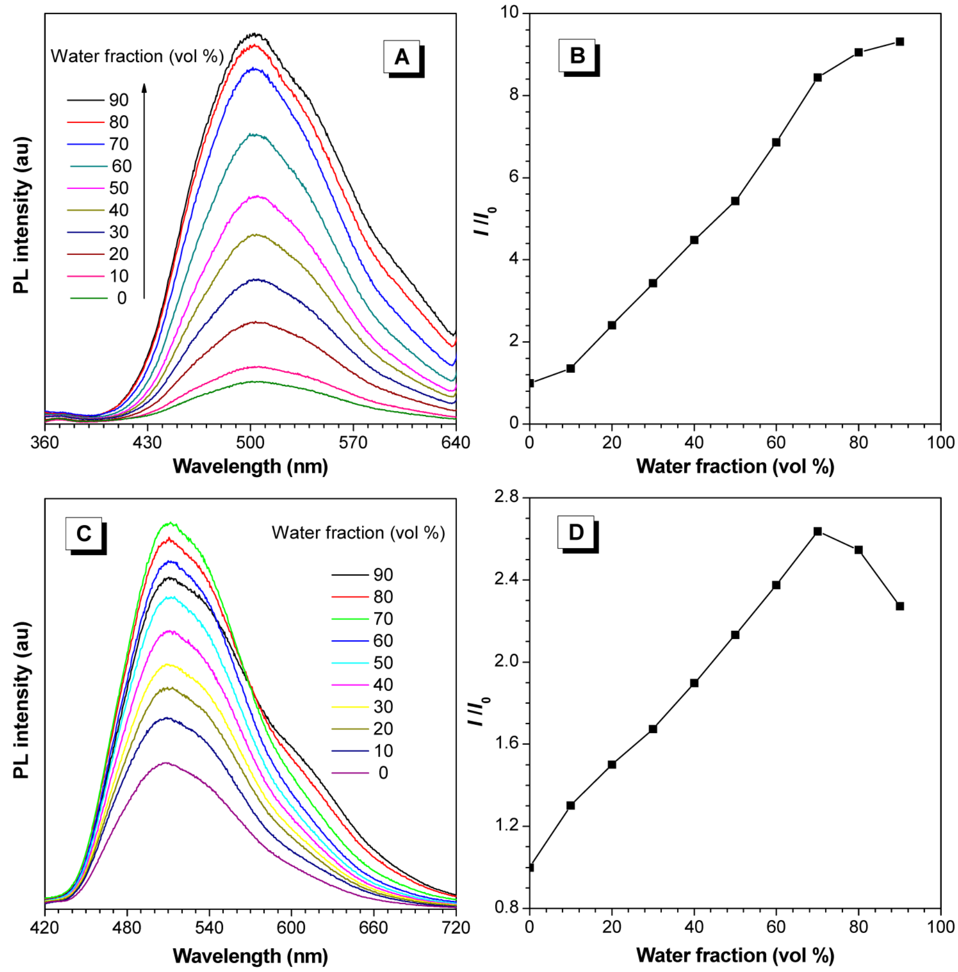

Figure 6. PL spectra of (A) P**1c**/**2**/**3** and (C) P**1e**/**2**/**3** in THF and THF/H_2O mixtures with different water fractions. Concentration: 10^{-5} M; excitation wavelength (nm): 335 (P**1c**/**2**/**3**) and 380 (P**1e**/**2**/**3**). (B, D) Plot of relative PL intensity (I/I_0) versus the composition of the THF/H_2O mixtures of P**1c**/**2**/**3** and P**1e**/**2**/**3**.

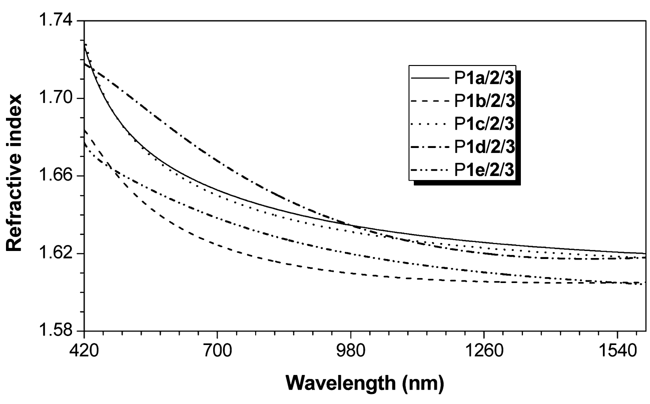

Figure 7. Wavelength dependence of refraction index of thin films of P**1a**–**e**/**2**/**3**.

Figure S1, all the ceramics consist of irregular nanoparticles (dark grains) wrapped by carboneous shell (light areas). Thermolysis of organic materials under nitrogen not only leads to the formation of carbon but also results in the evolution of volatile gases, such as methane and hydrogen. We therefore utilized XPS and EDX to determine the atomic compositions of the ceramics (Table 7). XPS study reveals the cobalt contents of 3.61, 4.28, 1.66, 1.56, and 2.26% on the surfaces of MC**1**–MC**5**, respectively. In the bulk, the values rise to 88.96, 37.64, 39.06, 82.49, and 49.93%, while opposite result was observed for the carbon content. This composition gradient from the bulk to the surface suggests that the ceramization process starts from the formation of cobalt nanocluster cores, which is then imbedded into a carbon matrix.

To further investigate the chemical structure of the bulk, we performed the XRD analysis. Figure 10 exhibits the XRD patterns of MC**1**–MC**5**. The reflection peaks can be identified according to the databases of JCPDS-International Centre for Diffraction Data (ICDD) as reflections for the Co metal (ICDD-data file 15-0806) and Co_2Si (ICDD-data file 04-0847). MC**1**–MC**5** all consist of a majority of Co. Particularly, MC**5** also contains a minority of Co_2Si nanocrystallites. This peak, however, is too weak to be observed in MC**2** though its precursor possesses Si atoms. The ED patterns of the Co nanoparticles show many diffraction spots (Figure 9D and Figure S2), indicating that the metal clusters are highly crystalline with well-ordered structures.

Magnetization. It now becomes clear that all the ceramic materials MC**1**–MC**5** contain nanoscopic cobalt species, which are expected to be magnetically susceptible. Figure 11 shows the magnetization curves of the ceramics. With an increase in the magnetic field strength, the magnetization of the ceramics MC**1**–MC**5** swiftly increases and a saturation magnetization (M_s) is ultimately reached. It is known that cobalt itself is

Table 6. Refractive Indices and Chromatic Dispersions of P1a–e/2/3[a]

polymer	n_{633}	n_{1550}	Δn_{633}	ν_D	ν_D'	D	D'
P1a/2/3	1.6603	1.6206	0.010	19.8	58.2	0.050	0.017
P1b/2/3	1.6317	1.6050	0.008	19.6	208.5	0.051	0.005
P1c/2/3	1.6581	1.6184	0.008	18.4	63.9	0.054	0.016
P1d/2/3	1.6791	1.6175	0.010	21.8	56.7	0.046	0.018
P1e/2/3	1.6448	1.6048	0.012	32.1	52.7	0.031	0.019

[a]Abbreviation: n = refractive index, Δn = birefringence, ν_D = Abbé number = $(n_D - 1)/(n_F - n_C)$, where n_D, n_F, and n_C are the RI values at wavelengths of 589.2, 486.1, and 656.3 nm, respectively, ν_D' = modified Abbé number = $(n_{1319} - 1)/(n_{1064} - n_{1550})$, where n_{1319}, n_{1064}, and n_{1550} are the RI values at 1319, 1064, and 1550 nm, respectively, $D^{(\prime)}$ = chromatic dispersion = $1/\nu_D^{(\prime)}$.

Scheme 4. Complexation with Cobalt Carbonyls and Ceramization to Magnetic Ceramics

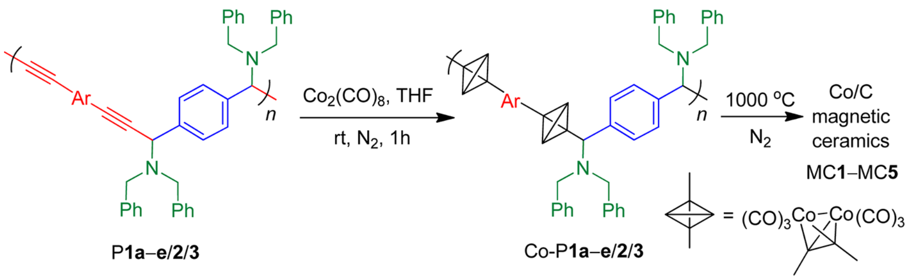

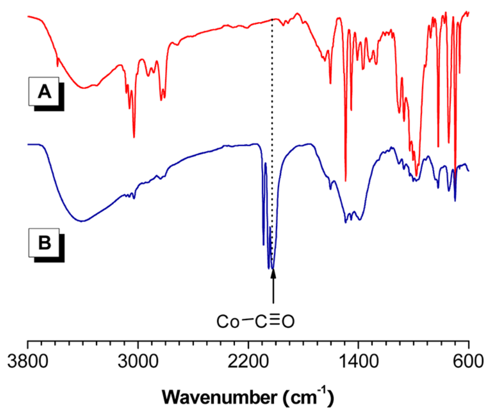

Figure 8. IR spectra of P1a/2/3 (A) before and (B) after complexation with $Co_2(CO)_8$.

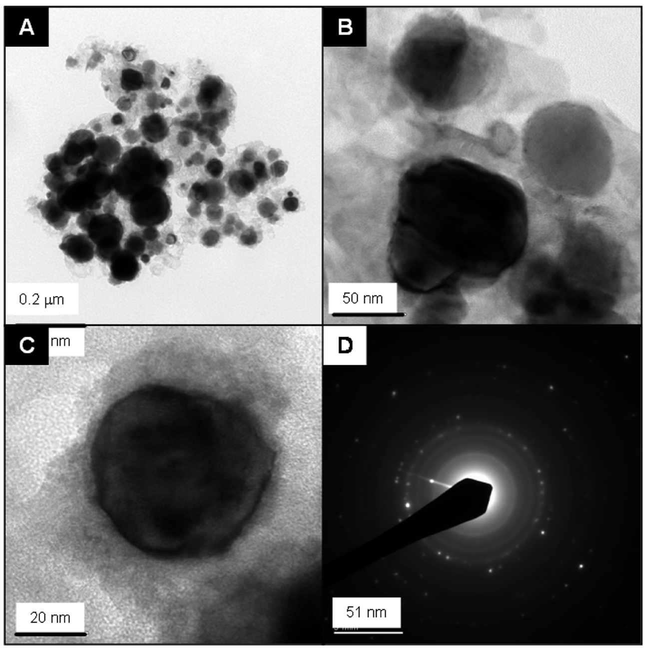

Figure 9. (A–C) TEM images and (D) ED pattern of the magnetic ceramics MC1.

ferromagnetic, but its oxides (Co_3O_4 and CoO) are paramagnetic at room temperature.[30] Among the magnetic ceramics, MC1 shows the highest M_s value of 80.7 emu/g, in agreement with its highest content of ferromagnetic Co nanocrystallites. This value is impressively high when taking into the account that the M_s value of maghemite (γ-Fe_2O_3) is 74 emu/g.[31] The carboneous shells may have well wrapped the cobalt nanocrystallites and prevent them from oxidation after the pyrolysis process. Comparing with MC1, the M_s values of MC2 (61.3 emu/g) and MC5 (61.2 emu/g) are lower because of their lower Co content but are still higher than those of MC3 (54.1 emu/g) and MC4 (56.4 emu/g) owing to the presence of a minority of paramagnetic Co_2Si.

The hysteresis loops of our magnetoceramics are small. From the enlarged H–M plots shown in the inset of Figure 11, the coercivities (H_c) of MC1–MC5 are found to be 0.19–0.21 kOe. Coupled with their high M_s values, they are anticipated to find an array of high-technological applications, especially in magnetic recording systems.

CONCLUSIONS

In this work, we developed a new polymerization route for the synthesis of new polymers with precise structures. The indium-catalyzed three-component polycouplings of diynes, dialdehyde, and secondary amine proceed smoothly in *o*-xylene at 140 °C for 20 h, producing polymers P1a–e/2/3 with high molecular weights in high yields. Rational model reaction was carried out to help elucidate the polymer structures. All the polymers possess good solubility and thermal stability. Whereas P1c/2/3 and P1e/2/3 exhibit an unusual AEE characteristics, others are ACQ emitters. This provides valuable information on how to build conjugated polymers with high emission efficiency in the

Table 7. Atomic Compositions of the Magnetic Ceramics Estimated by XPS and EDX Analyses

		XPS (atom %)				EDX (atom %)			
ceramics	yield[a] (%)	C	O	Si	Co	C	O	Si	Co
MC1	45.9	88.18	8.21		3.61	10.51	0.53		88.96
MC2	48.3	75.13	16.23	4.37	4.28	52.26	5.88	4.22	37.64
MC3	51.1	95.12	3.22		1.66	59.63	1.31		39.06
MC4	50.6	94.99	3.45		1.56	16.85	0.67		82.49
MC5	49.8	88.72	7.05	1.97	2.26	45.28	2.21	2.57	49.93

[a]Ceramics obtained by pyrolysis of Co−P**1a**−**e**/**2**/**3** at 1000 °C for 1 h under nitrogen.

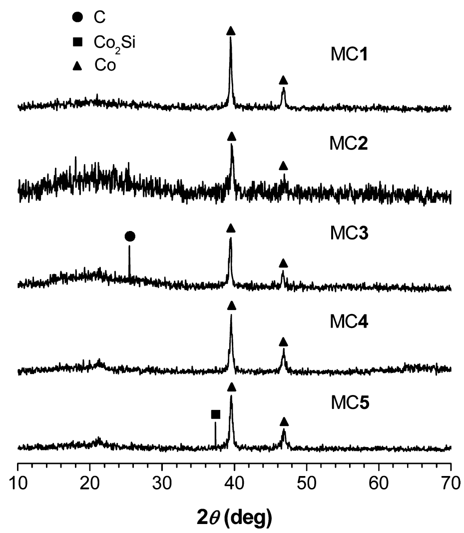

Figure 10. XRD diffractograms of the magnetic ceramics MC**1**−MC**5**.

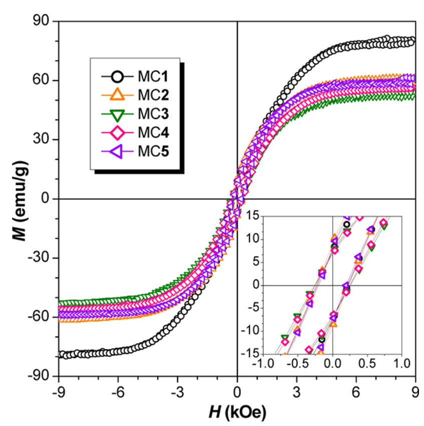

Figure 11. Plots of magnetization (M) versus applied magnetic field (H) at 298 K for magnetoceramics MC**1**−MC**5**. Inset: enlarged plots at low magnetic field.

Table 8. Magnetic Properties of the Ceramics[a]

ceramics	M_s (emu/g)	M_r (emu/g)	H_c (kOe)
MC1	80.7	8.4	0.20
MC2	61.3	10.4	0.19
MC3	54.1	8.0	0.21
MC4	56.4	7.6	0.20
MC5	61.2	9.6	0.20

[a]Determined by vibrating sample magnetometer. Abbreviation: M_s = saturation magnetization in an external field of ∼10 kOe, M_r = magnetic remanence at zero external field, and H_c = coercivity at zero magnetization.

aggregated state. All the polymer films show higher refractive indices than conventional organic polymers. The polymers can be utilized as processable precursors to magnetic ceramics. By complexation with $Co_2(CO)_8$ and pyrolysis of the resulting organometallic polymers at high temperature under inert atmosphere, nanostructured ceramics MC**1**−MC**5** with high magnetizability and low hysteresis loss are generated. We hope that the present results will inspire research enthusiasm for creation of new, precise polymers with new and/or enhanced functionalities and properties for high-technological applications in many areas.

■ ASSOCIATED CONTENT

Ⓢ Supporting Information

TEM images and ED patterns of the magnetic ceramics. This material is available free of charge via the Internet at http://pubs.acs.org.

■ AUTHOR INFORMATION

Corresponding Author

*E-mail chjacky@ust.hk (J.W.Y.L.) or tangbenz@ust.hk (B.Z.T.); Ph +852-2358-7375 (8801); Fax +852-2358-1594.

Notes

The authors declare no competing financial interest.

■ ACKNOWLEDGMENTS

This work has been partially supported by National Basic Research Program of China (973 Program; 2013CB834701), the Research Grants Council of Hong Kong (604711, 602212, HKUST2/CRF/10 and N_HKUST620/11), and the University Grants Committee of Hong Kong (AoE/P-03/08). B.Z.T. thanks the support of the Guangdong Innovative Research Team Program (201101C0105067115).

■ REFERENCES

(1) (a) For multi-component coupling reactions, see: *Multicomponent Reactions*; Zhu, J., Bienayme, H., Eds.; Wiley: Weinheim, 2005. (b) Ugi, I.; Domling, A.; Werner, B. *J. Heterocycl. Chem.* **2000**, *37*, 647−658. (c) Weber, L.; Illgen, K.; Almstetter, M. *Synlett* **1999**, 366−374. (d) Armstrong, R. W.; Combs, A. P.; Tempest, P. A.; Brown, S. D.; Keating, T. A. *Acc. Chem. Res.* **1996**, *29*, 123−131. (e) Ugi, I.; Steinbrueckner, C. *Chem. Ber.* **1961**, *94*, 2802−2814. (f) Mannich, C.; Kosche, W. *Arch. Pharm.* **1912**, *250*, 647−667. (g) Hantzsch, A. *Ber. Dtsch. Chem. Ges.* **1890**, *23*, 1474−1476. (h) Strecker, A. *Ann. Chem.* **1850**, *75*, 27−45.

(2) (a) Bienayme, H.; Hulme, C.; Oddon, G.; Schmitt, P. *Chem.—Eur. J.* **2000**, *6*, 3321−3329. (b) Bienayme, H.; Bouzid, K. *Angew. Chem., Int. Ed.* **1998**, *37*, 2234−2237. (c) Trost, B. M. *Angew. Chem., Int. Ed.* **1995**, *34*, 259−281.

(3) Lalli, C.; Bouma, J. M.; Bonne, D.; Masson, G.; Zhu, J. *Chem.—Eur. J.* **2011**, *17*, 880−889.

(4) Li, C.-J.; Wei, C. *Chem. Commun.* **2002**, 268−269.

(5) Chen, W.-W.; Bi, H.-P.; Li, C.-J. *Synlett* **2010**, *3*, 475−479.

(6) Dou, X.-Y.; Shuai, Q.; He, L.-N.; Li, C.-J. *Adv. Synth. Catal.* **2010**, *352*, 2437−2440.

(7) Zhang, Y.; Li, P.; Wang, M.; Wang, L. *J. Org. Chem.* **2009**, *74*, 4364−4367.

(8) (a) Ishibe, S.; Tomita, I. *J. Polym. Sci., Part A: Polym. Chem.* **2005**, *43*, 3403−3410. (b) Choi, C.-K.; Tomita, I.; Endo, T. *Macromolecules* **2000**, *33*, 1487−1488. (c) Choi, C.-K.; Tomita, I.; Endo, T. *Chem. Lett.* **1999**, 1253−1254. (d) Miyaki, N.; Tomita, I.; Endo, T. *Macromolecules* **1997**, *30*, 4504−4506. (e) Miyaki, N.; Tomita, I.; Endo, T. *J. Polym. Sci., Part A: Polym. Chem.* **1997**, *35*, 1211−1218. (f) Miyaki, N.; Tomita, I.; Endo, T. *Macromolecules* **1996**, *29*, 6685−6690.

(9) Ochiai, B.; Ogihara, T.; Mashiko, M.; Endo, T. *J. Am. Chem. Soc.* **2009**, *131*, 1636−1637.

(10) (a) Wang, Y.-Z.; Deng, X.-X; Li, L.; Li, Z.-L.; Du, F.-S.; Li, Z.-C. *Polym. Chem.* **2013**, *4*, 444−448. (b) Li, L.; Kan, X.-W.; Deng, X.-X.; Song, C.-C.; Du, F.-S.; Li, Z.-C. *J. Polym. Sci., Part A: Polym. Chem.* **2013**, *51*, 865−873.

(11) (a) Liu, J.; Lam, J. W. Y.; Tang, B. Z. *Chem. Rev.* **2009**, *109*, 5799−5867. (b) Häußler, M.; Tang, B. Z. *Adv. Polym. Sci.* **2007**, *209*, 1−58.

(12) (a) Lam, J. W. Y.; Tang, B. Z. *Acc. Chem. Res.* **2005**, *38*, 745−754. (b) Li, Z.; Dong, Y.; Qin, A.; Lam, J. W. Y.; Dong, Y.; Yuan, W.; Sun, J.; Hua, J.; Wong, K. S.; Tang, B. Z. *Macromolecules* **2006**, *39*, 467−469. (c) Li, Z.; Dong, Y.; Häussler, M.; Lam, J. W. Y.; Dong, Y.; Wu, L.; Wong, K. S.; Tang, B. Z. *J. Phys. Chem. B* **2006**, *110*, 2302−2309. (d) Zeng, Q.; Lam, J. W. Y.; Jim, C. K. W.; Qin, A.; Qin, J.; Li, Z.; Tang, B. Z. *J. Polym. Sci., Part A: Polym. Chem.* **2008**, *46*, 8070−8080.

(13) (a) Häußler, M.; Lam, J. W. Y.; Qin, A.; Tse, K. K. C.; Li, M. K. S.; Liu, J.; Jim, C. K. W.; Gao, P.; Tang, B. Z. *Chem. Commun.* **2007**, 2584−2586. (b) Häußler, M.; Zheng, R.; Lam, J. W. Y.; Tong, H.; Dong, H.; Tang, B. Z. *J. Phys. Chem. B* **2004**, *108*, 10645−10650.

(14) (a) Liu, J.; Zhong, Y.; Lam, J. W. Y.; Lu, P.; Hong, Y.; Yu, Y.; Yue, Y.; Faisal, M.; Sung, H. H. Y.; Williams, I. D.; Wong, K. S.; Tang, B. Z. *Macromolecules* **2010**, *43*, 4921−4936. (b) Jim, C. K. W.; Qin, A.; Lam, J. W. Y.; Häußler, M.; Liu, J.; Yuen, M. M. F.; Kim, J. K.; Ng, K. M.; Tang, B. Z. *Macromolecules* **2009**, *42*, 4099−4109.

(15) (a) Qin, A.; Lam, J. W. Y.; Tang, B. Z. *Chem. Soc. Rev.* **2010**, *39*, 2522−2544. (b) Qin, A.; Lam, J. W. Y.; Tang, B. Z. *Macromolecules* **2010**, *43*, 8693−8702.

(16) (a) Jim, C. K. W.; Qin, A.; Lam, J. W. Y.; Faisal, M.; Yu, Y.; Tang, B. Z. *Adv. Funct. Mater.* **2010**, *20*, 1319−1328. (b) Liu, J.; Lam, J. W. Y.; Jim, C. K. W.; Ng, J. C. Y.; Shi, J.; Su, H.; Yeung, K. F.; Hong, Y.; Faisal, M.; Yu, Y.; Wong, K. S.; Tang, B. Z. *Macromolecules* **2011**, *44*, 68−79.

(17) Lu, P.; Lam, J. W. Y.; Liu, J.; Jim, C. K. W.; Yuan, W.; Chan, C. Y. K.; Xie, N.; Hu, Q.; Cheuk, K. K. L.; Tang, B. Z. *Macromolecules* **2011**, *44*, 5977−5986.

(18) Liu, J.; Deng, C.; Tseng, N.-W.; Chan, C. Y. K.; Yue, Y.; Ng, J. C. Y.; Lam, J. W. Y.; Wang, J.; Hong, Y.; Sung, H. H. Y.; Williams, I. D.; Tang, B. Z. *Chem. Sci.* **2011**, *2*, 1850−1859.

(19) Li, Z.; Qin, A.; Lam, J. W. Y.; Dong, Y.; Dong, Y.; Ye, C.; Williams, I. D.; Tang, B. Z. *Macromolecules* **2006**, *39*, 1436−1442.

(20) (a) Liu, J.; Zheng, R.; Tang, Y.; Haussler, M.; Lam, J. W. Y; Qin, A.; Ye, M.; Hong, Y.; Gao, P.; Tang, B. Z. *Macromolecules* **2007**, *40*, 7473−7486. (b) Peng, H.; Cheng, L.; Luo, J.; Xu, K.; Sun, Q.; Dong, Y.; Salhi, F.; Lee, P. P. S.; Chen, J.; Tang, B. Z. *Macromolecules* **2002**, *35*, 5349−5351.

(21) Birks, J. B. *Photophysics of Aromatic Molecules*; Wiley: London, 1970.

(22) (a) Hong, Y.; Lam, J. W. Y.; Tang, B. Z. *Chem. Soc. Rev.* **2011**, *40*, 5361−5388. (b) Liu, Y.; Tang, Y.; Barashkov, N. N.; Irgibaeva, I. S.; Lam, J. W. Y.; Hu, R.; Yu, Y.; Tang, B. Z. *J. Am. Chem. Soc.* **2010**, *132*, 13951−13953. (c) Yuan, W. Z.; Lu, P.; Chen, S.; Lam, J. W. Y.; Wang, Z.; Liu, Y.; Kowk, H. S.; Ma, Y.; Tang, B. Z. *Adv. Mater.* **2010**, *22*, 2159−2163. (d) Zhao, Z.; Wang, Z.; Lu, P.; Chan, C. Y. K.; Liu, D.; Lam, J. W. Y.; Sung, H. H. Y.; Williams, I. D.; Ma, Y.; Tang, B. Z. *Angew. Chem., Int. Ed.* **2009**, *48*, 7608−7611. (e) Hong, Y.; Lam, J. W. Y.; Tang, B. Z. *Chem. Commun.* **2009**, 4332−4353. (f) Luo, J. D.; Xie, Z. L.; Lam, J. W. Y.; Cheng, L.; Chen, H. Y.; Qiu, C. F.; Kwok, H. S.; Zhan, X. W.; Liu, Y. Q.; Zhu, D. B.; Tang, B. Z. *Chem. Commun.* **2001**, 1740−1741.

(23) Chen, H. Y.; Lam, W. Y.; Luo, J. D.; Ho, Y. L.; Tang, B. Z.; Zhu, D. B.; Wong, M.; Kwok, H. S. *Appl. Phys. Lett.* **2002**, *81*, 574−576.

(24) Liu, J.; Ueda, M. *J. Mater. Chem.* **2009**, *19*, 8907−8919 and references therein.

(25) (a) Seferis, J. C. *Polymer Handbook*, 3rd ed.; Brandrup, J., Immergut, E. H., Eds.; Wiley: New York, 1989; pp VI/451−VI/461. (b) Mills, N. J. *Concise Encyclopedia of Polymer Science & Engineering*; Kroschwitz, J. I., Ed.; Wiley: New York, 1990; pp 683−687.

(26) Hecht, E. *Optics*, 4th ed.; Addison Wesley: San Francisco, CA, 2002.

(27) (a) Burchell, T. J.; Puddephatt, R. J. *Inorg. Chem.* **2005**, *44*, 3718−3730. (b) Eisler, D. J.; Puddephatt, R. J. *Cryst. Growth Des.* **2005**, *5*, 57−59. (c) Mohr, F.; Jennings, M. C.; Puddephatt, R. J. *Angew. Chem., Int. Ed.* **2004**, *43*, 969−971. (d) Burchell, T. J.; Eisler, D. J.; Jennings, M. C.; Puddephatt, R. J. *Chem. Commun.* **2003**, 2228−2229. (e) Puddephatt, R. J. *Macromol. Symp.* **2003**, *196*, 137−144. (f) Qin, Z. Q.; Jennings, M. C.; Puddephatt, R. J.; Muir, K. W. *Inorg. Chem.* **2002**, *41*, 5174−5186. (g) Hunks, W. J.; Jennings, M. C.; Puddephatt, R. J. *Inorg. Chem.* **2002**, *41*, 4590−4598. (h) Hunks, W. J.; Jennings, M. C.; Puddephatt, R. J. *Chem. Commun.* **2002**, 1834−1835. (i) Brandys, M. C.; Puddephatt, R. J. *J. Am. Chem. Soc.* **2002**, *124*, 3946−3950. (j) Qin, Z. Q.; Jennings, M. C.; Puddephatt, R. J. *Chem. Commun.* **2002**, *4*, 354−355.

(28) (a) Bill, J.; Aldinger, F. *Adv. Mater.* **1995**, *7*, 775−787. (b) Interrante, L. V.; Liu, Q.; Rushkin, I.; Shen, Q. *J. Organomet. Chem.* **1996**, *521*, 1−10. (c) Corriu, R. J. P. *Angew. Chem., Int. Ed.* **2000**, *39*, 1376−1398. (d) Manners, I. *Science* **2001**, *294*, 1664−1666.

(29) (a) Babudri, F.; Farinola, G. M.; Naso, F. *J. Mater. Chem.* **2004**, *14*, 11−34. (b) Chan, W. Y.; Berenbaum, A.; Clendenning, S. B.; Lough, A. J.; Manners, I. *Organometallics* **2003**, *22*, 3796−3808. (c) Long, N. J.; Williams, C. K. *Angew. Chem., Int. Ed.* **2003**, *42*, 2586−2617. (d) Bunz, U. H. F. *J. Organomet. Chem.* **2003**, *683*, 269−287.

(30) (a) O'Handley, R. C. *Modern Magnetic Materials: Principles and Applications*; Wiley: New York, 2000. (b) Goldmann, A. *Handbook of Ferromagnetic Materials*; Kluwer: Boston, MA, 1999. (c) Evetts, J. E. *Concise Encyclopedia of Magnetic & Superconducting Materials*; Pergamon: New York, 1992.

(31) (a) Tang, B. Z.; Geng, Y.; Lam, J. W. Y.; Li, B.; Jing, X.; Wang, X.; Wang, F.; Pakhomov, A. B.; Zhang, X. X. *Chem. Mater.* **1999**, *11*, 1581−1589. (b) Tang, B. Z. *CHEMTECH* **1999**, *29* (11), 7−12. (c) Tang, B. Z.; Geng, Y.; Sun, Q.; Zhang, X.; Jing, X. *Pure Appl. Chem.* **2000**, *72*, 157−162.